15. S. V. Stenovskii, *Zh. Prikl. Mekh. Tekh. Fiz.*, No. 1, 89-92 (1979).
16. J.F. Bitten and E. G. Fochtman, *AIChE J.*, **9**, No. 2, 279-282 (1963).
17. G. I. Den'shchikova, Yu. V. Goryunov, and B. D. Summ, *Vestnik MGU, Ser. 2, Khim.* **18**, No. 4, 419-422 (1977).
18. N. I. Smirnov and S. E. Polyuta, *Zh. Prikl. Khim.*, **21**, No. 11, 1137-1146 (1948).
19. V. B. Okhotskii, *Inzh.-Fiz. Zh.*, **54**, No. 2, 203-211 (1988).

NUMERICAL AND PHYSICAL SIMULATION OF AXISYMMETRIC STREAMLINING OF A STAGED CYLINDER WITH A LOW-VELOCITY FLOW OF AIR

S. A. Isaev, V. M. Suprun, and O. A. Shul'zhenko

UDC 532.517.4

The mechanism to reduce the frontal resistance to the motion of a staged cylinder of circular cross section and limited length is analyzed on the basis of a numerical solution for the Reynolds equations closed by means of a dissipative two-parameter model of turbulence, and through systematic measurement in wind tunnels.

1. Achieving organized or predictable flow separation in the vicinity of streamlined surfaces, from the standpoint of conceptual aerohydrodynamics, is possible in a variety of ways, some of which are discussed in [1]. There is no doubt that the multiplicity of possible situations does not exhaust the material contained in [1], all the more so because primary attention is devoted to an examination of long bodies of revolution. At the same time, practical requirements dictate a broadening of the spectrum of geometric configurations in bodies and, in particular, call for an analysis of the streamlining of short bodies and of bodies that are not circular in lateral cross section, examples of which can be found among the containers used in aviation, maritime, and railroad transport, trailers used in trucking, floating drilling platforms, and the like (see, for example, [2]).

The frontal resistance in poorly streamlined bodies is achieved by locating protrustions of various shapes across the surfaces of these bodies, or by positioning these bodies in the near wake, behind other bodies. In the present study the mechanism used to reduce resistance of bodies during the formation of the leading separation zone, as analyzed in detail in [1] for a cylinder with a protruding disk, using the examples of bodies with considerably simpler geometry, we examine a staged cylinder of circular lateral cross section and of limited length. We should note that the aerodynamics of short cylinders with coaxially positioned disks in the leading and rear areas is presented in [3].

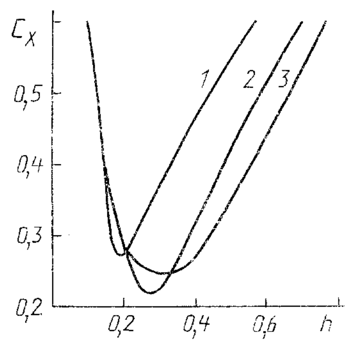

Fig. 1. Experimental functions relating the coefficient of frontal resistance C_x for a stepped cylinder to the step height h for elongations of the protrusion in the step portion of l = 0.2 (1), 0.4 (2), 0.6 (3).

Academy of Civil Aviation, Leningrad. Translated from Inzhenerno-Fizicheskii Zhurnal, Vol. 60, No. 3, pp. 433-439, March, 1991. Original article submitted March 14, 1990.

0022-0841/91/6003-0342$12.50

TABLE 1. Expression for the Unknown Variable, the Coefficients of Transfer, and the Source Term in Eq. (1)

Φ	Γ_Φ	S_Φ
1	0	0
u	ν_{eff}	$\frac{1}{y}\left\{\frac{\partial}{\partial x}\left(\nu_{eff}\, y \frac{\partial u}{\partial x}\right) + \frac{\partial}{\partial y}\left(\nu_{eff}\, y \frac{\partial v}{\partial x}\right)\right\} - \frac{\partial}{\partial x}\left(p + \frac{2}{3}k\right)$
v	ν_{eff}	$\frac{1}{y}\left\{\frac{\partial}{\partial x}\left(\nu_{eff}\, y \frac{\partial u}{\partial y}\right) + \frac{\partial}{\partial y}\left(\nu_{eff}\, y \frac{\partial v}{\partial y}\right)\right\} - \frac{\partial}{\partial y}\left(p + \frac{2}{3}k\right) - 2\nu_{eff}\frac{v}{y^2}$
k	$\frac{1}{Re} + \frac{\nu_t}{\sigma_k}$	$P - \varepsilon$
ε	$\frac{1}{Re} + \frac{\nu_t}{\sigma_\varepsilon}$	$\frac{\varepsilon}{k}\left(C_{\varepsilon 1} P - C_{\varepsilon 2}\, \varepsilon\right)$

Note. $\nu_{eff} = 1/Re + \nu_t$; $\nu_t = C_\mu f_\mu k^2/\varepsilon$; $f_\mu = 1/(1 + C_c \cdot Ri_t)$; $P = \nu_t = \{2(\partial u \partial x)^2 + 2(\partial v/\partial y)^2 + 2(v/y)^2 + (\partial u/\partial y + \partial v/\partial x)^2\}$.

The entire apparatus of physical and numerical modeling methods is used successively and in coordinated fashion (as if to correct and verify one method against the other, on the one hand, and respectively enhancing each other on the other hand). At the same time, an approach used extensively in [1] has undergone subsequent development in a number of other complex studies (see, for example, [3]).

2. The experimental study of the streamlining of staged-cylinder models by means of a low-velocity flow of air was undertaken in a closed-type of wind tunnel with an open work space of circular cross section. The coefficient of frontal resistance was measured on a staged cylinder with an elongation of $\lambda = 3$ by means of Prandtl lever-type balances (all linear dimensions are referred to the radius of the cylinder). In the parametric study the effect of the geometric dimensions for the protruding cylindrical portion of the model on the coefficient C_x of frontal resistance and on the pattern of separation flow the stage height h and its length l were varied in limited of h = 0-0.6 and l = 0-0.8. The Reynolds number determined from the velocity of the flow through the working section of the tunnel and the radius of the cylinder was $Re = 1.2 \cdot 10^5$. For purposes of comparison, we examined cylindrical bodies of equal elongation and various aerodynamic shapes, among which were included a cylinder with a forward protruding disk and a cylinder which held a hollow cylinder (a ring) of smaller diameter on the leading forward surface, as well as a cylinder with a well-streamlined nose section.

The aerodynamic experiment follows standard techniques. The error in the determination of C_x did not exceed 5%. The level of flow turbulence in the working section of the tunnel amounted to 0.5%. The correction factor for the encumbering of the flow by the model, calculated on the basis of the method presented in [4], amounted to 3% and was taken into account in estimating C_x. Visualization of the vortex structure encountered in the streamlining of the model was accomplished by the silk-thread method and by the liquid-film method, which involved introduction of coloring agent onto the surface of the model. The streamlining test experiment on a short cylinder with a flat edge provided good agreement between the derived results for the components of the coefficient of frontal resistance with existing characteristics from earlier studies (see, for example, [5]): the profile resistance amounted to 80% of the frontal resistance of the model ($C_x^p \simeq 0.65$), the bottom resistance amounted to 18% ($C_{xd} \simeq 0.15$), and the frictional resistance came to 2% ($C_{xf} \simeq 0.02$).

Figure 1 shows some results from physical experiments on the effect of the step height h on the frontal resistance factor C_x of the stepped cylinder for several step lengths l. Analysis of the functions $C_x(h, l)$ indicates the existence of an optimum frontal resistance for a stepped-cylinder assembly analogous to the one investigated in [1], exhibiting the configuration of a cylinder with a protruding forward disk. Minimum frontal resistance is exhibited by a cylinder with a step characterized by the following dimensions: h = 0.27, l = 0.4, where $C_{x_{min}} = 0.21$. This assembly is virtually equivalent in terms of frontal resistance to the optimum disk—cylinder configuration with a disk radius R = 0.75 of the cylinder radius, and a gap of L = 0.75 between the disk and the cylinder, for which a magnitude of $C_x = 0.22$ has been determined experimentally. The optimum step-cylinder configuration is also close in terms of frontal resistance to the assembly of a cylinder with a ring having dimensions of h = 0.31 and l = 0.4 ($C_x = 0.20$), as well as to a cylinder with a well-streamlined leading portion elongated through 2 radii of the cylinder ($C_x = 0.19$). It is important to point

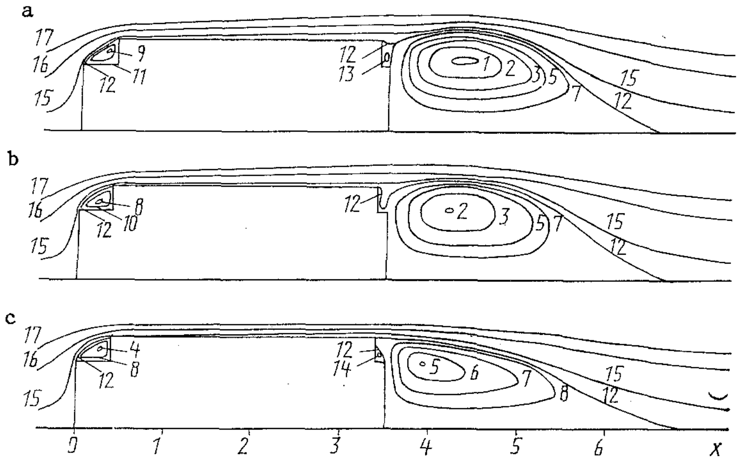

Fig. 2. Theoretical streamlining patterns optimum from the standpoint of frontal resistance for the stepped-cylinder configuration in a laminar regime at Reynolds numbers of Re = $2 \cdot 10^3$ (a), $2 \cdot 10^4$ (b), and in the turbulent regime at Re = $2 \cdot 10^5$ (c): a) $\psi = -0.10$; 2) (−0.08); 3) (−0.06); 4) (−0.05); 5) (−0.04); 6) (−0.03); 7) (−0.02); 8) (−0.01); 9) (−0.006); 10) (−0.002); 11) (−0.001); 12) 0; 13) 0.001; 14) 0.002; 15) 0.01; 16) 0.1; 17) 0.2.

TABLE 2. Standard Semiempirical Constants for a Dissipative Two-Parameter Turbulent Model

C_μ	σ_k	σ_ε	C_{ε_1}	C_{ε_2}	C_c
0,09	1,0	1,3	1,45	1,92	0,1

out the interrelationship between the presence of a resistance-optimum step-cylinder assembly and the vortex structure with which such a cylinder is streamlined. Flow visualization shows that minimum resistance is exhibited by such a body of revolution when the separation zone is localized in the space between the sharp leading edge and the trailing face of the cylinder, with attachment of the flow directly in the limited area provided by the sharp edge of the cylinder. Such a streamline pattern corresponds to smooth flow along the side surface of the cylinder, which is characteristic, as is well known, of bodies with smooth forward shape.

As follows from the comparative analysis that we have carried out with respect to the streamlining of bodies exhibiting various configurations, of greatest interest is a detailed study of the streamlining of a stepped cylinder of optimum geometry. The information derived in the physical experiment is exceedingly incomplete, limited as to the number of measured parameters. In order to expand the spectrum of flow characteristics examined, in particular to include in it the local flow parameters and turbulence characteristics, we undertook a numerical simulation of axisymmetric streamlining of a body of optimum geometry ($h = 0.27$, $l = 0.4$) with the intent of reproducing the conditions of the physical experiment.

3. The steady axisymmetric streamlining of such a stepped cylinder with a flow of an incompressible viscous fluid was calculated on the basis of solving the Navier–Stokes equations written in cylindrical coordinates (x, y) by a finite-difference method for the case of a laminar flow regime and Reynolds equations closed by means of a dissipative two-parameter turbulence model for the turbulent regime. The system of equations written in divergent form for the generalized variable Φ (Φ = u, v, k, ε) has the form

$$\frac{1}{y}\left[\frac{\partial}{\partial x}(yu\Phi)+\frac{\partial}{\partial y}(yv\Phi)-\frac{\partial}{\partial x}\left(\Gamma_\Phi\, y\,\frac{\partial\Phi}{\partial x}\right)-\frac{\partial}{\partial y}\left(\Gamma_\Phi\, y\,\frac{\partial\Phi}{\partial y}\right)\right]=S_\Phi\,. \tag{1}$$

The quantities contained in Eq. (1) and in the source term have been tabulated in Table 1. Table 2 shows the turbulent characteristics for the transfer equation, as well as the semiempirical constants in the expression for the coefficient of turbulent viscosity ν_t. A modified k–ε model of turbulence was used in this study to account for the effect of streamline curvature on the turbulence characteristics within the framework of the Leshtsiner–Rodi approach. The additionally introduced semiempirical constant C_c in the function relating the coefficient of turbulent viscosity to the turbulent Leshtsiner number has been chosen through a special methodological study detailed in [1]. A set of near-wall functions has been used in the calculations.

The finite-difference algorithm for the solution of the problem is based on the concept of separating the physical processes. The modified Reitbi and Van Durmal SIMPLEC pressure-correction procedure is used in the construction of this algorithm, said procedure characterized by features which, in contrast to the standard version, involve the utilization of equations (to approximate the convective terms) exhibiting low numerical diffusion of the quadratic Leonard counterflow scheme and the solution of a system

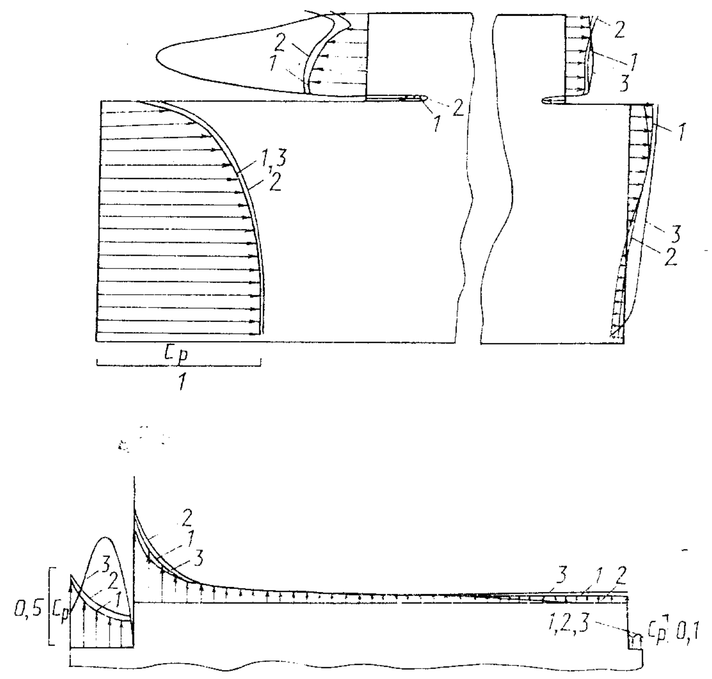

Fig. 3. Static-pressure distributions over the surface of a stepped cylinder ($h = 0.27$, $l = 0.4$) calculated at Reynolds numbers of Re = $2{\cdot}10^3$ (curves 1), $2{\cdot}10^4$ (2), and $2{\cdot}10^5$ (3).

TABLE 3. Theoretical and Measured Coefficients of Frontal Resistance and Its Components for a Cylinder of Limited Length ($\lambda = 3$) with a Staged Nose Section ($h = 0.27$, $l = 0.4$)

Coefficient of frontal resistance and its components	Results of calculations			Measurement data
	Laminar flow regime		Turbulent flow regime	
	Re			
	$2{\cdot}10^3$	$2{\cdot}10^4$	$2{\cdot}10^5$	$2{,}3{\cdot}10^5$
C_x	0,710	0,460	0,220	0,210
C_{xp}	0,295	0,280	0,040	0,040
C_{x1}^{p}	0,415	0,430	0,420	—
C_{x2}^{p}	—0,120	—0,150	—0,380	—
C_{xd}	0,115	0,120	0,155	0,150
C_{xf}	0,300	0,060	0,025	0,020

of algebraic equations by the Buleev method of incomplete matrix factorization in the SIP variant of the Stone method. The detailed test studies conducted in [1] demonstrated that these features of the calculation algorithm produce acceptable accuracy and efficiency in the numerical simulation of complex separation flows. Let us note that the convergence of the computational process is controlled through satisfaction of the conditions of constancy (with a specified accuracy of order 10^{-3}) in the frontal resistance coefficient C_x and through the unchangeability of local turbulence characteristics at selected points.

4. Calculations dealing with the streamlining of a stepped cylinder which exhibits optimum configuration in terms of frontal resistance were carried out with the laminar (Re = $2{\cdot}10^3$ and $2{\cdot}10^4$) and turbulent (Re = $2{\cdot}10^5$) regimes. In the latter case, we reproduce the conditions of the physical experiments in a wind tunnel and, in particular, we specified the corresponding magnitudes of turbulence for the oncoming incident flow and the scale of the energy-bearing vortices. A checkerboard pattern was used in the numerical study, with the nodes distributed so as to congregate near the sharp edges. The minimum interval in the region of large gradients for the parameters defining the flow amounted to 0.02. Approximately 1 h of processing time on an ES-1045 computer was needed to solve the problem of the turbulent streamlining of a stepped body on a grid containing on the order of 2000 nodes.

Figures 2-4 and Table 3 show some of the described results. Analysis of the streamlining spectra for the body under consideration, for the pressure profiles, and for the profiles of the axial velocity component, demonstrates the evolution of the separation flow

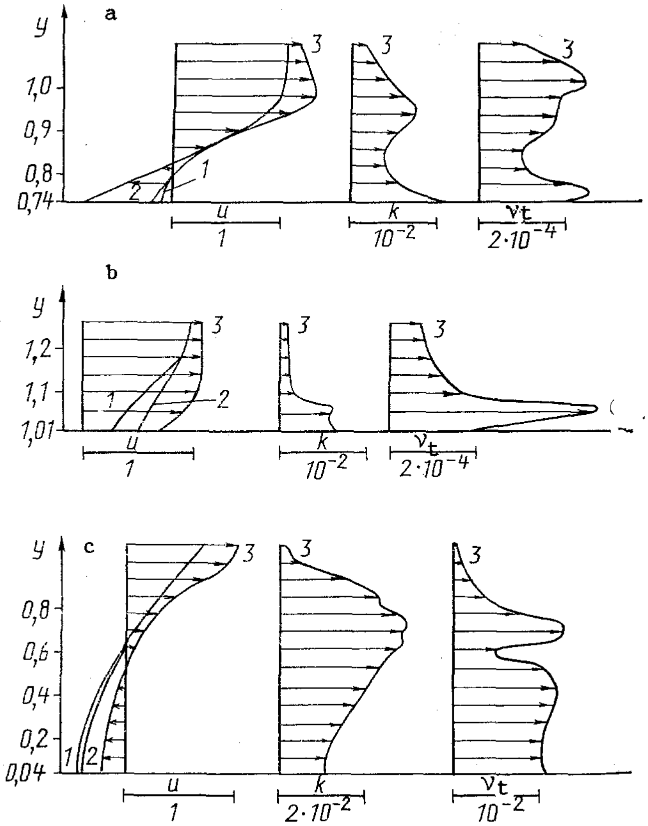

Fig. 4. Profiles of the longitudinal component of velocity u, the energy k of turbulent pulsations, and the turbulent viscosity ν_t, calculated at the lateral cross sections x = 0.2 (a), 2 (b), 5 (c): 1) Re = $2 \cdot 10^3$; 2) $2 \cdot 10^4$; 3) $2 \cdot 10^5$.

as the Reynolds number increases. It is important to note the constancy in the configuration of the leading separation zone over a broad range of variations in the Re number, which is determined by the fixed position of the separation points and the reattachment of the flow near the sharp leading edges of the step nose section. The intensity of the large-scale vortex increases in this case, and this is evidenced by the increase in the maximum magnitude of the stream function in its core from 0.006 for Re = $2 \cdot 10^3$ to 0.049 for Re = $2 \cdot 10^5$. As a consequence, rarefaction is intensified at the leading base of the cylinder (from $C_{P_{min}} = -0.35$ for Re = $2 \cdot 10^3$ to $C_{P_{min}} = -1.27$ when Re = $2 \cdot 10^5$), which results in the sharp reduction in the profile resistance of the body, and in the frontal resistance of that body, to a considerable extent. It is interesting to note that the maximum velocity of the reverse flow in the vortex turns out to be commensurate with the velocity of the incident flow, as was noted in [1] in an examination of the turbulent streamlining of a cylinder with a forward disk. The coefficient of profile resistance for such a step body ($C_{xp} = 0.04$) is very close to the analogous coefficient of the optimum "disk—cylinder" assembly ($C_{xp} = 0.031$).

The evolution of flow in the near wake behind the body, as the Reynolds number increases, proceeds in a conventional manner that is similar to the process of flow formation behind a cylinder of considerable elongation. This is a consequence of the straightening of the flow near the side surface of a cylinder of rather small elongation, associated with the organization of the leading separationzone. The reverse effect of the flow in the near wake behind the body on the forward separation zone goes virtually unnoticed. It is meaningful to indicate the significant difference between the large-scale vortex structures in the forward portion of the body, as opposed to those behind the body, both in terms of flow circulation intensity and turbulent characteristics. The flow in the forward separation zone is characterized by comparatively low levels of turbulent energy and vortical turbulent viscosity. Conversely, the flow in the wake is distinguished by the great magnitudes of turbulent viscosity, exceeding by an order or more the quantity ν_t in the forward vortex.

The comparative analysis of the computational results and physical experiments with respect to the coefficient of frontal resistance and its components indicates their good agreement. This latter circumstance serves as yet another validation (in addition to the one presented in [1]) of the suitability of this computational algorithm, as developed here, and furthermore, doubtlessly increases the reliability with which the derived experimental data are regarded. In conclusion, let us point out that the coefficients of frontal resistance to the motion of an optimum stepped-body assembly can be estimated approximately 10% lower than the values shown in the table as a consequence of the distorting effect on the structure of the separation streamlining and on C_x for the level of flow turbulence in the operational section of the wind tunnel [1].

NOTATION

x and y, axial and radial coordinates; h, step height; l, length of protruding step portion; λ, length of cylindrical portion of stepped body; R and L, radius of disk and clearance between disk and cylinder in the "disk—cylinder" assembly; u and v, axial and radial components of velocity; C_p, coefficient of static pressure, excess relative to the pressure in the incident flow; ψ, stream function; k, turbulence energy; ε, rate of turbulent energy dissipation; ν_t, coefficient of turbulent viscosity; Re, Reynolds number; C_x, C_{xp}, C_{xd}, and C_{xf}, coefficients of frontal, profile, bottom resistance, and frictional resistance; $C_{x1}{}^p$ and $C_{x2}{}^p$, components of profile resistance, governed by the staged portion and end surfaces of the cylinder; Ri_t, turbulent Richardson number. Subscripts: min, minimum.

LITERATURE CITED

1. I. A. Belov, S. A. Isaev, and V. A. Korobkov, *Problems and Methods of Calculating Separation Flows for an Incompressible Fluid* [in Russian], Leningrad (1989).
2. T. Lajos, *Wind Eng. Indust. Aerodyn.,* **22**, 331-338 (1986).
3. I. A. Belov, I. M. Dement'ev, S. A. Isaev, et al., "Analysis of results and methodological validation of modeling the streamlining of bodies with a forward separation zone," Preprint No. 1353, Physicotechnical Institute, Leningrad (1989).
4. T. Morel and M. Bon, *Teor. Osnovy Inzh. Raschetov,* **102**, No. 1, 225-234 (1980).
5. S. M. Gorlin, *Experimental Aerodynamics* [in Russian], , Moscow (1970).